

Segmentation of Imagery Using Network Snakes

MATTHIAS BUTENUTH, Hannover

Keywords: Computer vision, segmentation, imagery, snakes, network, topology, shape

Zusammenfassung: Bildsegmentierung mit Hilfe von network snakes. Der Beitrag beschreibt eine neue Methodik zur Segmentierung von Bildern mit network snakes. Snakes stellen ein bekanntes Verfahren zur Detektion von Objekten dar, welches jedoch auf geschlossene Objektkonturen begrenzt ist. Dieser Beitrag erweitert das Verfahren und fokussiert auf Objekte, die ein Netzwerk bilden bzw. Objekte, die benachbart und nur durch eine Grenzlinie getrennt sind. Zusätzlich liegt der Fokus auf linearen Objekten mit offenen, nicht fixierten Enden. Die interne Energie, die die Form des Objektes während des Energieminimierungsprozesses beschreibt, ist für unterschiedliche Knotengrade definiert, um die Topologie des Objektes ausnutzen zu können. Exemplarische Ergebnisse zeigen die Funktionsweise und Übertragbarkeit der vorgestellten Methode: Zunächst werden Schlaggrenzen aus hoch aufgelösten Satellitenbildern extrahiert. Das zweite Beispiel aus dem Medizinbereich befasst sich mit der Abgrenzung von Zellen in Zellgewebeaufnahmen. Abschließend werden einige Anmerkungen zu der vorgestellten Methodik gemacht und zukünftige Arbeiten diskutiert.

Abstract: A new methodology for the segmentation of imagery using network snakes is presented in this paper. Snakes are a well known technique, but usually are limited to closed object boundaries. Enhancing traditional snakes the focus is on objects forming a network respectively being adjacent with only one boundary in between. In addition, the focus is on linear objects with open non-fixed endings. The internal energy controlling the shape of the object contours during the energy minimization process is defined for nodes with different degrees to enable the exploitation of the object topology. Exemplary results of two different applications demonstrate the functionality and transferability of the proposed methodology: First, field boundaries are extracted from high resolution satellite imagery. The second example from the medical sector deals with the delineation of adjacent cells in microscopic cell imagery. Concluding remarks are given at the end to point out further investigations.

1 Introduction

The segmentation of imagery is a well known problem in image processing and computer vision. One important methodology to delineate objects precisely are active contours, first introduced by (KASS et al. 1988). Active contours are a sophisticated image processing technique combining image features with shape constraints in an energy minimization process. Parametric active contours, often called snakes (KASS et al. 1988, BLAKE & ISARD 1998), have a rigid

topology, in contrary to geometric active contours (MALLADI et al. 1995, CASELLES et al. 1997), which are able to change their topology due to flexible level sets and thus allow for extracting foreground objects without prior knowledge about their shape. Numerous approaches using snakes have been presented to detect different objects in many kinds of imagery, for example refer to medical image segmentation (MCINERNEY & TERZOPoulos 1996, SURI et al. 2002), 3D deformable surface models (COHEN & COHEN 1993), the extraction of roads using

scale space and snakes (LAPTEV et al. 2000) or the displacement of lines in cartographic generalization tasks (BURGHARDT & MEIER 1997).

Most of these approaches require closed contours, which describe the boundary of an object separately – a limitation concerning linear objects with open non-fixed endings and a limitation regarding objects, which form a network and thus interact with each other during the optimization process. A new methodology of parametric active contours to overcome these restrictions is presented in this paper, called network snakes. In the literature, only a limited amount of work can be found regarding active contours beyond explicitly or implicitly represented closed object boundaries. Trihedral corners imposing constraints of 90 degree angles between the three edges ending at the corner are used to extract buildings in (FU et al. 2000). An extension of parametric active contours, which combines the ability to handle transiently touching objects and exerts topological control is given in (ZIMMER & OLIVIO-MARIN 2005). An adaptive adjacency graph consisting of a network of active contours was firstly introduced in (JASIOBEDZKI 1993) and afterwards utilized in (DICKINSON et al. 1994) to track 3D objects. The authors introduce constraints in the form of springs to connect the contour ends, but the approach does not enable the definition of a unique nodal point including a geometrical control of the contours up to the nodal point.

In contrary, the methodology presented in this paper is able to handle objects with a given network topology, but without the necessity of introducing any particular constraints. Possible applications using network snakes are, for example, the extraction of road networks, field boundaries as well as adjacent cells. For these purposes parametric active contours are more applicable than level set techniques, since the image-dependent energy terms of parametric active contours are defined specifically to individual objects. Multiple level sets as well as multiple parametric active contours are not suitable, because they can intersect or over-

lay each other losing the correct topology. However, parametric active contours need an initialization to start the energy minimization process. The required information can be taken from an initial segmentation or from a GIS, as long as a correct topology can be assumed.

The next section outlines traditional snakes, while Section 3 focuses on the enhancements concerning network snakes. In Section 4 exemplary results of two different applications are presented to demonstrate the potential and the transferability of the proposed methodology: At first, the extraction of field boundaries from high resolution satellite imagery is depicted. Field boundaries have become objects of increasing interest during the last few years. Application areas are geo-scientific questions such as the derivation of potential wind erosion risk fields and applications in the agricultural sector, for instance precision farming or the monitoring of subsidies. Work on the extraction of field boundaries exists but is limited, for example refer to (TORRE & RADEVA 2000, APLIN & ATKINSON 2004), but neither a fully automatic solution nor the exploitation of the topology is used. The second exemplary result highlighted in Section 4 is the extraction of adjacent cells in microscopic cell imagery. Medical image segmentation has received a large attention, in particular the delineation of cells for high-throughput biological research and drug discovery (SURI et al. 2002, JONES et al. 2005). However, the focus is mostly on single cells not taking into account the neighborhood. Finally, concluding remarks are given and further investigations are discussed in Section 5.

2 Traditional snakes

In this section, parametric active contours are summarized in order to provide a basis for a discussion of their pros and cons concerning the enhancements contained in Section 3. Traditional snakes (KASS et al. 1988) are defined as a parametric curve

$$v(s) = (x(s), y(s)) \quad (1)$$

where s is the arc length and x and y are the image coordinates of the 2D-curve. In the simplest way, the image energy can be written as the image intensity itself with

$$E_{img}(v(s)) = I(v(s)) \quad (2)$$

where I represents the image. In the literature, the image energy is often defined as

$$E_{img}(v(s)) = -|\nabla I(v(s))|^2 \quad (3)$$

$|\nabla I(v(s))|$ is the norm or magnitude of the gradient image at the coordinates $x(s)$ and $y(s)$. In practice, the image energy $E_{img}(v(s))$ is computed by integrating the values $|\nabla I(v(s))|$, taken from precomputed gradient magnitude images along the line segments, that connect the vertices of the contour. The internal energy is defined as

$$E_{int}(v(s)) = \frac{1}{2}(\alpha(s) \cdot |v_s(s)|^2 + \beta(s) \cdot |v_{ss}(s)|^2) \quad (4)$$

where v_s and v_{ss} are the first and second derivative of v with respect to s . The function $\alpha(s)$ controls the first-order term of the internal energy: the elasticity. When the aim is to minimize $E_{int}(v(s))$ and $v(s)$ is allowed to move, large values of $\alpha(s)$ let the contour become very straight between two points. The function $\beta(s)$ controls the second-order term: the rigidity. Large values of $\beta(s)$ let the contour become smooth, small values allow the generation of corners. $\alpha(s)$ and $\beta(s)$ need to be predefined based on the modeled shape characteristics of the object of interest.

The total energy of the snake E_{snake}^* , to be minimized, is defined as

$$\begin{aligned} E_{snake}^* &= \int_0^1 E_{snake}(v(s)) ds \\ &= \int_0^1 [E_{img}(v(s)) + E_{int}(v(s)) + E_{con}(v(s))] ds \end{aligned} \quad (5)$$

The additional external energy $E_{con}(v(s))$ is introduced in (KASS et al. 1988) as an external constrained force, which provides the opportunity for individual forces at particu-

lar parts or points of the contour. With constant weight parameters $\alpha(s) = \alpha$ and $\beta(s) = \beta$ a minimum of the total energy in Equation 5 can be derived by solving the Euler equation:

$$\frac{\partial E_{img}(v(s))}{\partial v(s)} - \alpha v_{ss}(s) + \beta v_{ssss}(s) = 0 \quad (6)$$

The derivatives are approximated with finite differences since they can not be computed analytically. Converted to vector notation with $v_i = (x_i, y_i)$ and with $\partial E_{img}(v(s))/\partial v(s) = f_v(v)$ the Euler equations read

$$\begin{aligned} &\alpha_i(v_i - v_{i-1}) - \alpha_{i+1}(v_{i+1} - v_i) \\ &+ \beta_{i-1}(v_{i-2} - 2v_{i-1} + v_i) \\ &- 2\beta_i(v_{i-1} - 2v_i + v_{i+1}) \\ &+ \beta_{i+1}(v_i - 2v_{i+1} + v_{i+2}) \\ &+ f_v(v) = 0 \end{aligned} \quad (7)$$

and can be rewritten in matrix form as

$$Av + f_v(v) = 0 \quad (8)$$

A is a pentadiagonal matrix, which depends only on the functions α and β . Equation 8 can be solved iteratively by introducing a step size γ multiplied with the negative time derivatives $\partial v/\partial t$, which are discretized by $v_t - v_{t-1}$. It is assumed that $f_v(v)$ is constant during a time step, i. e. $f_v(v_t) \approx f_v(v_{t-1})$, yielding an explicit Euler step regarding the image energy. In contrast, the internal energy is an implicit Euler step due to their specification by the banded matrix A . The resulting equation is

$$Av_t + f_v(v_{t-1}) = -\gamma(v_t - v_{t-1}) \quad (9)$$

The time derivatives vanish at the equilibrium ending up in Equation 8. Finally, a solution can be derived by matrix inversion:

$$v_t = (A + \gamma I)^{-1}(\gamma v_{t-1} - \kappa f_v(v_{t-1})) \quad (10)$$

where I is the identity matrix and κ is an additional parameter in order to control the weight between internal and image energy.

A requirement of traditional snakes is the necessity to have an initialization close to the true object boundary. Additional terms

to increase the capture range of the image forces and thus bridge larger gaps between initialization and true object boundary, for example the balloon model (COHEN 1991), are only applicable, when the background is relatively homogeneous and no disturbing structures hinder the movement of the snake. Since these conditions can not be guaranteed in general, a solution without such additional terms is preferred in this work. Instead, strong internal energies are used containing the modeled shape characteristics of the object of interest to be relatively independent of the initialization and those parts of the image energies, which represent disturbing structures.

3 Network snakes

In order to enhance traditional snakes to be able to deal with network topologies and open endings of contours, a closer look to the internal energy $E_{int}(v(s))$ controlling the shape part of the curve is required. The minimization of the internal energy during the optimization process is only defined for closed object boundaries, i.e. $v_0 = v_n$ (KASS et al. 1988), because the derivatives are approximated with finite differences (cf. Equation 7). Most of the approaches to be found in the literature use closed contours or define fixed end points when using open contours. This process requires correct end points before starting the snake optimization, which often can not be guaranteed. Similarly, network topologies represented by single con-

tours ending in common nodal points require predefined correct nodal points. In this work a new definition of snakes is given, achieving a solution using image features and shape constraints without fixed end or nodal points.

At first, the topology of the initial contour has to be derived. In addition to the nodes with a degree $\rho(v) = 2$ of the preliminary contour $v(s)$ each node with a degree $\rho(v) \neq 2$ has to be set up. Nodes with a degree $\rho(v) = 1$ define the end points and nodes with a degree $\rho(v) \geq 3$ define the nodal points of the contour (cf. Fig. 1 for an example).

Imposing the network topology in the energy minimization process causes a problem when solving Equations 7 and 8: the derivatives approximated by finite differences are not defined for nodes with a degree $\rho(v) = 1$ or $\rho(v) \geq 3$, because the required neighboring nodes are either not available ($\rho(v) = 1$) or existing multiple times ($\rho(v) \geq 3$). Thus, the shape control can not be accomplished at these parts of the contour in a traditional way.

Let v_a , v_b and v_c represent three contours, each ending in a common *nodal point* v_n with a degree $\rho(v) = 3$. Regarding Equation 7, the first term, weighted by the parameter α , can not support the control of the internal energy during the energy minimization process in the vicinity of v_n when using network snakes: the finite differences of the first term approximating the derivatives are only available for the two nodes v_{n-1} and v_n , but not for v_{n+1} . Thus, no shape control is possible and the first term is not considered. The second term of the internal energy, weighted by the parameter β , is rewritten using the available finite differences controlling the curvature of the contour. Consequently, the control of the total energy at the common nodal point $v_n = v_{a_n} = v_{b_n} = v_{c_n}$ is defined for network snakes as follows:

$$\begin{aligned}\beta(v_{a_n} - v_{a_{n-1}}) - \beta(v_{a_{n-1}} - v_{a_{n-2}}) + f_{v_a}(v_a) &= 0 \\ \beta(v_{b_n} - v_{b_{n-1}}) - \beta(v_{b_{n-1}} - v_{b_{n-2}}) + f_{v_b}(v_b) &= 0 \\ \beta(v_{c_n} - v_{c_{n-1}}) - \beta(v_{c_{n-1}} - v_{c_{n-2}}) + f_{v_c}(v_c) &= 0\end{aligned}\quad (11)$$

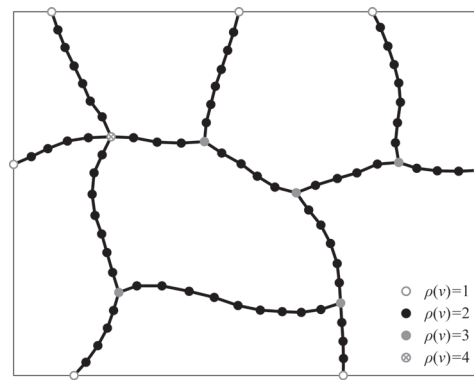


Fig. 1: Topology of a network snake.

All three contours intersect in the common nodal point without interacting concerning their particular shape. The energy definition of Equation 11 allows for a minimization process controlling the shape of each contour separately, though ending in one common point exploiting the network topology. The matrix A of Equation 8 is adapted accordingly at the nodal points and their neighbors to fulfill the new definition of the internal energy, i. e. omitting some parts of the banded structure and/or filling up some additional parts to build further connections between different parts of the contour.

The definition of the internal energy for nodes with a degree $\rho(v) > 3$ is straightforward to the proposed method above, i. e. adding further parts to Equation 11. Similarly, the new internal energy is defined at the *end points* of a contour: only one part of Equation 11 is needed, because only one contour without connection to other parts of the contour is available. The adaptation of the matrix A is analogous compared to nodal points. Thus, the control of the shape is feasible by the end of the contour without fixing the end points.

Snakes have the tendency to shorten during the energy minimization due to the first term (α -term) of Equation 4. A shortening of contours with an open ending can be avoided by chaining the end points at the image border allowing for movement only along the image borders (cf. Fig. 1). Alternatively, the contour can be chained at a topologically neighbored object allowing for movement only along the object border. When there are no neighbored objects to allow for chaining the open endings of the contour, a possible idea could be the introduction of an external constraint force regarding a constant length of the contour.

4 Exemplary results

Results concerning the functionality and capability of network snakes are presented in this section. Two different applications are shown to point out the transferability of the methodology: the extraction of field boundaries from high resolution satellite imagery

and the extraction of cells from microscopic cell imagery.

4.1 Extraction of field boundaries

The delineation of field boundaries within the complex environment of vegetation is accomplished with color satellite images having a resolution of two meters. The strategy for extracting the objects of interest is divided into two parts: First, a segmentation is carried out in a coarse scale to derive the topology taking into account a somewhat inaccurate geometrical position. The topology of the segmentation, however, is assumed to be correct. In a second step, network snakes are used to improve the preliminary results exploiting the local image features and the object topology.

The initial segmentation of the imagery is briefly outlined below, for details refer to (BUTENUTH & HEPKE 2005). The use of prior knowledge from a GIS enables a partition of the image scene: Field boundaries are only located within the open landscape and, in addition, the road network describes already fixed field boundaries, because fields naturally end at these objects. Within these regions of interest a multi-channel region growing is performed using the RGB- and IR-channels of the image resulting in an initial segmentation of the image (cf. Fig. 2a, blue lines). Note, that the geometrical correctness of the segmentation has been artificially degraded to emphasize the following steps in a better way.

The result of the segmentation is used to derive the topology (cf. Fig. 2b) and to initialize the network snake. Since the objects to be extracted are rather straight, the parameter β is set to a large value compared to α . Thus, image noise and small disturbances have relatively small effects and, in addition, relatively coarse initial values of the contour can be used. The open endings of the contour are chained to the image borders, and are allowed for movement only along the borderline. In Fig. 2c the capability of the network snake is highlighted: the contours and in particular the nodal points with a degree $\rho(v) \geq 3$ and the end points move to

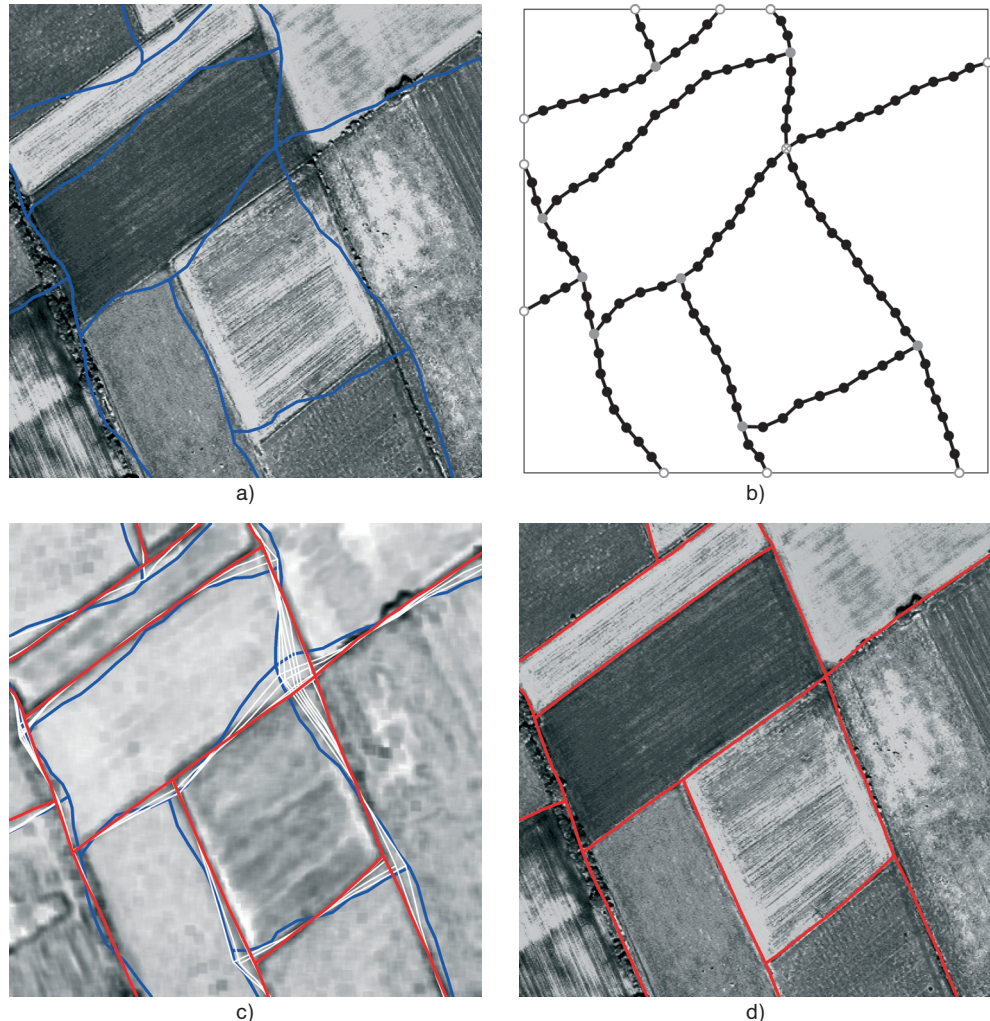


Fig. 2: Extraction of field boundaries from high resolution satellite imagery (400×400 pixels): a) initialization of the network snake (blue); b) topology; c) initialization (blue), movement (white) and result of the snake (red); d) result superimposed on the intensity channel of the CIR-image.

the correct result, although the initialization is rather poor. The underlying image consists of the standard deviation of the image intensities of the CIR-image within a quadratic mask, because high values typically belong to field boundaries. Regarding the area around the nodal points, in particular the point with a degree $\rho(v) = 4$, the internal energy and the exploitation of the topology specify the movement of the contour during the first iteration steps, because the values

of the image energy are without effect. Step by step, the inverted image energy helps with small values pushing the contour respectively the nodal points to the correct solution during the minimization process. The final result is depicted in Fig. 2d superimposed on the satellite image. The geometrical correctness is in most parts convincing, only the tree rows on the left side prevent a clearly defined field boundary and, thus, the image energy can not support the energy minimi-

zation process in an optimal manner. However, the example demonstrates, network snakes are a powerful methodology to delineate objects precisely exploiting their topology.

4.2 Extraction of cells

The delineation of adjacent cells in microscopic cell imagery is the second example presented in this section. Fig. 3a shows a microscopic image of stained cytoplasm, which fluoresced during the data capture. The depicted image has a size of about 20×20 micrometers. Again, the strategy for extracting the objects of interest is divided into two parts: At first, a coarse object contour is needed to initialize the processing and to derive the topology. In a subsequent step the geometrical correctness of the initial object contour is optimized using network snakes.

The cell nuclei are much easier to detect than the boundaries of the cytoplasm (cell membrane), because they are well defined against the background (cf. Fig. 3b). The background of the cell nuclei image is segmented followed by a calculation of the skeleton (cf. Fig. 3b, blue line). Due to the fact, that each cell nucleus is located within the associated cell membrane, the skeleton can be used to initialize the network snake having a correct topology even though the geometrical correctness is not very high. Before starting the optimization process, the object contour is thinned out taking into account an equal distance between each node (cf. Fig. 3c, blue line).

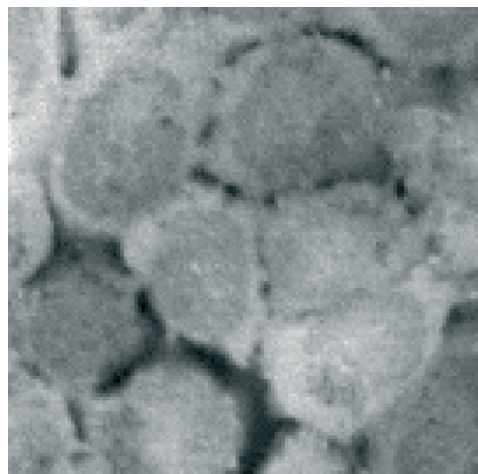
The topology of the object contour is derived to set up the network snake (cf. Fig. 3d). Since the objects to be extracted have a specific curvature, the parameter β controlling the internal energy of the energy minimization process is not set to such a large value compared to the extraction of mostly straight field boundaries (cf. Section 4.1), yet is set again larger than α . A histogram linearization of the original image is accomplished to ease the optimization, because the enhanced contrast of the image helps to push the contour to the correct solu-

tion. In Fig. 3e the optimization process is highlighted: Starting from the initialization (blue line) the movement of the network snake (white line) is depicted resulting in extracted cell boundaries (red line). In Fig. 3f the final result is superimposed on the cell image. The optimization process works well, although there is strong image noise and in parts the image intensities can not help yielding the correct result. In the lower right part of the image one cell is not delineated completely, because the initialization is too far away and the image energy is not able to push the contour to the true object boundary.

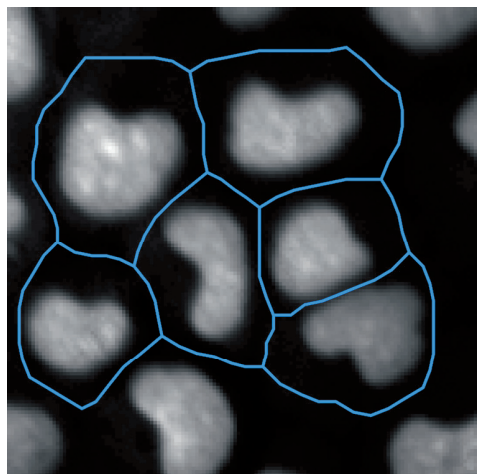
5 Conclusions

A new segmentation methodology to delineate objects precisely from imagery using network snakes is presented in this paper. Using traditional snakes, adjacent objects, which influence each other and objects forming a network or having open endings are not defined due to the representation of the internal energy. In contrary, network snakes exploit the topology of the objects of interest during the energy minimization process comprising a complete shape control of the contours. The exploitation of the topology turns out to be a powerful method to deal with noise and disturbances in the imagery. The obtained object contours represent a superior geometrical solution when interacting with each other compared to traditional snakes.

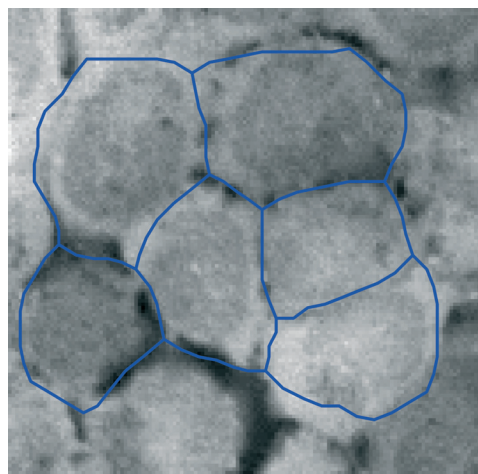
Different results concerning the extraction of field boundaries from high resolution satellite imagery and the extraction of cells from microscopic cell imagery demonstrate the potential and the transferability of the proposed methodology. In addition, the two examples emphasize, the requirement of a given correct topology can be achieved in particular applications. However, when the assumption of a given correct topology can not be guaranteed, an additional intervention comprising the global view of the optimized network has to be considered to insert or delete parts of the contour. Possible further applications are the delineation of



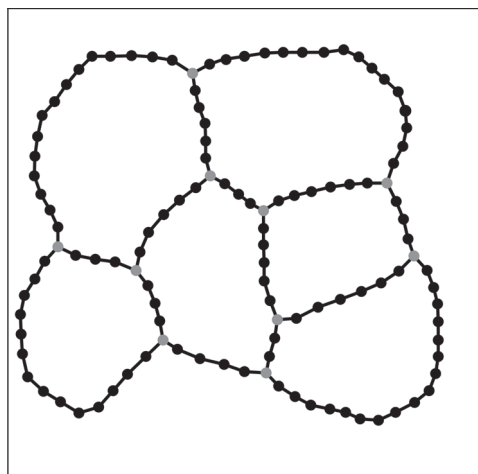
a)



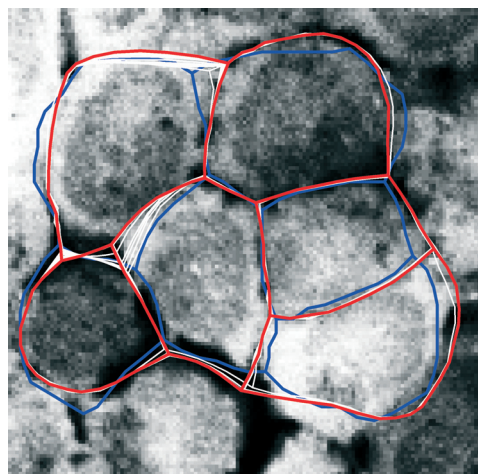
b)



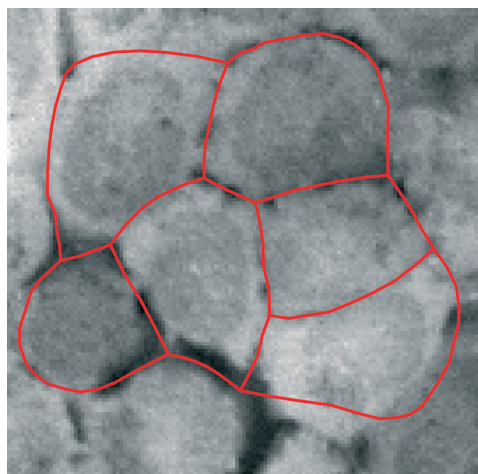
c)



d)



e)



f)

◀ **Fig. 3:** Extraction of cells from microscopic cell imagery (135×135 pixels): a) cell image; b) cell nuclei and derived initialization (blue); c) initialization of the network snake (blue); d) topology; e) initialization (blue), movement (white) and result of the snake (red); f) result superimposed on cell image [imagery provided by Evotec Technologies].

other objects such as road networks, and other topics such as the update of GIS-data with an already given topology.

In addition, the control of the internal energy can be improved choosing varying values of the parameters α and β , if the modeled object shape has these characteristics. A further interesting question is the behavior of the iteration process: are there dependencies of the initialization, internal energy and image characteristics and can they be exploited? For example, if the object of interest has other shape characteristics than the image disturbances or noise, the control of the internal energy and the exploitation of the topology can allow for a relatively coarse initialization. Investigations regarding this problem can give specific answers about the required quality of the image data and the initialization.

References

- APLIN, P. & ATKINSON, P.M., 2004: Predicting Missing Field Boundaries to Increase Per-Field Classification Accuracy. – Photogrammetric Engineering & Remote Sensing **70** (1): 141–149.
- BLAKE, A. & ISARD, M., 1998: Active Contours. – 351 p., Springer Verlag, Berlin Heidelberg New York.
- BURGHARDT, D. & MEIER, S., 1997: Cartographic Displacement Using the Snake Concept. – In: FÖRSTNER & PLÜMER (eds.): Semantic Modeling for the Acquisition of Topographic Information from Images and Maps. – Birkhäuser Verlag, Basel, pp. 59–71.
- BUTENUTH, M. & HEIPKE, C., 2005: Network Snakes-Supported Extraction of Field Boundaries from Imagery. – In: KROPATSCH, SABLATTNIG & HANBURY (eds.): Pattern Recognition. – Lecture Notes in Computer Science **3663**: 417–424, Springer-Verlag.
- CASELLES, V., KIMMEL, R. & SAPIRO, G., 1997: Geodesic Active Contours. – International Journal of Computer Vision **22** (1): 61–79.
- COHEN, L.D. & COHEN, I., 1993: Finite Element Methods for Active Contour Models and Balloons for 2-D and 3-D Images. – IEEE Transactions on Pattern Analysis and Machine Intelligence **15** (11): 1131–1147.
- COHEN, L.D., 1991: On Active Contour Models and Balloons. – CVGIP: Image Understanding **53** (2): 211–218.
- DICKINSON, S.J., JASIOBEDZKI, P., OLOFSSON, G. & CHRISTENSEN, H.I., 1994: Qualitative Tracking of 3-D Objects Using Active Contour Networks. – Proceedings IEEE Conference on Computer Vision and Pattern Recognition, Seattle, pp. 812–817.
- FUA, P., GRÜN, A. & LI, H., 2000: Optimization-Based Approaches to Feature Extraction from Aerial Images. – In: DERMANIS, GRÜN & SANZO (eds.): Geomatic Methods for the Analysis of Data in the Earth Sciences. – Lecture Notes in Earth Science **95**: 190–228, Springer Verlag.
- JASIOBEDZKI, P., 1993: Adaptive Adjacency Graphs. – SPIE **2031**, Geometric Methods in Computer Vision II, pp. 294–303, San Diego.
- JONES, T.R., CARPENTER, A. & GOLLAND, P., 2005: Voronoi-Based Segmentation of Cells on Image Manifolds. – In: LIU, JIANG & ZHANG (eds.): Lecture Notes in Computer Science **3765**, pp. 535–543, Springer Verlag.
- KASS, M., WITKIN, A. & TERZOPOLUS, D., 1988: Snakes: Active Contour Models. – International Journal of Computer Vision **1**: 321–331.
- LAPTEV, I., MAYER, H., LINDEBERG, T., ECKSTEIN, W., STEGER, C. & BAUMGARTNER, A., 2000: Automatic Extraction of Roads from Aerial Images Based on Scale Space and Snakes. – Machine Vision and Applications **12**: 23–31.
- MALLADI, R., SETHIAN, J.A. & VEMURI, B.C., 1995: Shape Modeling with Front Propagation: A Level Set Approach. – IEEE Transactions on Pattern Analysis and Machine Intelligence **17** (2): 158–175.
- MCINERNEY, T. & TERZOPoulos, D., 1996: Deformable Models in Medical Image Analysis: A Survey. – Medical Image Analysis **1** (2): 91–108.
- SURI, J.S., KAMALEDIN SETAREHDAN, S. & SINGH, S., 2002: Advanced Algorithmic Approaches to Medical Image Segmentation: State-of-the-Art Applications in Cardiology, Neurology, Mammography and Pathology. – 668 p., Springer Verlag, Berlin Heidelberg New York.

- TORRE, M. & RADEVA, P., 2000: Agricultural Field Extraction from Aerial Images Using a Region Competition Algorithm. – International Archives of Photogrammetry and Remote Sensing **XXXIII** (B2): 889–896.
- ZIMMER, C. & OLIVIO-MARIN, J.C., 2005: Coupled Parametric Active Contours. – IEEE Transactions on Pattern Analysis and Machine Intelligence **27** (11): 1838–1842.

Address of the author:

Dipl.-Ing. MATTHIAS BUTENUTH
Institut für Photogrammetrie und
GeoInformation
Leibniz Universität Hannover
Nienburger Str. 1, D-30167 Hannover
e-mail: butenuth@ipi.uni-hannover.de

Manuskript eingereicht: November 2006
Angenommen: November 2006